metals

MDPI

Article

Selective Separation and Recovery of Li from Spent $LiFePO_4$ Cathode Materials by Oxidation Roasting Followed by Low-Acid Pressure Leaching

Zaoming Chen [1,2], Changquan Shen [1], Fupeng Liu [1,2,*] and Jinliang Wang [1,2]

[1] Faculty of Materials Metallurgy and Chemistry, Jiangxi University of Science and Technology, Ganzhou 341000, China; 9120040042@jxust.edu.cn (Z.C.); 18370477088@163.com (C.S.); simwjl@163.com (J.W.)

[2] Jiangxi Provincial Key Laboratory of Flash Green Development and Recycling, Jiangxi University of Science and Technology, Ganzhou 341000, China

* Correspondence: fupengliu@126.com; Tel.: +86-1887-979-6708; Fax: +86-0797-831-2422

Abstract: The environmental and economic benefits of recycling spent $LiFePO_4$ batteries are becoming increasingly important. Nevertheless, the reprocessing of this type of material by conventional processes remains a challenge due to the difficulties of Li and Fe separation and low product purity. Herein, a new approach for recovering Li to separate iron and phosphorus from spent $LiFePO_4$ cathode materials is developed. Selective separation of Li can be achieved by oxidation roasting followed by low-acid pressure leaching. During the oxidation-roasting stage, almost all the stable $LiFePO_4$ cathode materials were first transformed into $Li_3Fe_2(PO_4)_3$ and Fe_2O_3, with the most suitable oxidation-roasting temperature determined to be 550 °C. Then, >96% of Li could be extracted using 0.5 mol·L^{-1} H_2SO_4 with an L/S ratio of 150 g·L^{-1} at 110 °C for 1 h; in contrast, the leaching of Fe was 0.03%. The mineral-phase composition of the leaching residues mainly includes $FePO_4 \cdot 2H_2O$, Fe_2O_3, and C, which can be used as a raw material for preparing battery-grade $FePO_4$. These findings demonstrate that the recycling process has the advantages of high selectivity for Li, excellent reaction kinetics, low acid consumption, and free oxidizing agent that may benefit the development of a circular economy.

Keywords: spent $LiFePO_4$; low-acid pressure leaching; oxidation roasting; selective recovery

check for updates

Citation: Chen, Z.; Shen, C.; Liu, F.; Wang, J. Selective Separation and Recovery of Li from Spent $LiFePO_4$ Cathode Materials by Oxidation Roasting Followed by Low-Acid Pressure Leaching. *Metals* **2023**, *13*, 1884. https://doi.org/10.3390/met13111884

Academic Editor: Denise Crocce Romano Espinosa

Received: 8 October 2023
Revised: 10 November 2023
Accepted: 10 November 2023
Published: 13 November 2023

Copyright: © 2023 by the authors. Licensee MDPI, Basel, Switzerland. This article is an open access article distributed under the terms and conditions of the Creative Commons Attribution (CC BY) license (https://creativecommons.org/licenses/by/4.0/).

1. Introduction

Lithium-ion batteries have drawn attention worldwide since their commercialization by Sony in 1991 [1]. They are widely applied in computers, communication, consumer electronics (3C), electric vehicles (EVs), and large-scale storage systems [2,3]. It has been forecasted that the global consumption of lithium-ion batteries will expand from approximately 8 million in 2019 to 50 million by 2025 and close to 140 million by 2030; these increases correspond to an annual average growth rate of close to 30% [3,4]. Olivine-structured lithium iron phosphate batteries ($LiFePO_4$) have attracted significant attention for their inherent advantages of excellent safety, thermal stability, low cost, low toxicity, and long lifecycle [5,6]. Due to the wide applications and rapid increase in $LiFePO_4$ cathode materials, particularly in China, the total number of retired $LiFePO_4$ batteries will significantly increase within the next decade. Apparently, it is necessary to develop recovery techniques for Li, Fe, and P from spent $LiFePO_4$ batteries and further prepare battery-grade $FePO_4$ and Li_2CO_3 to resynthesize $LiFePO_4$ cathode materials [7].

To date, numerous studies have focused on two main methods for recycling spent $LiFePO_4$, direct regeneration and utilization of $LiFePO_4$ cathodes, in which a proper amount of raw materials is added to spent $LiFePO_4$ cathodes on the basis of the needed molar ratio of Li, Fe, and P through the high-temperature solid-phase synthesis of new $LiFePO_4$ [8–10]. According to the cost calculation, spent $LiFePO_4$ can yield a profit after direct regeneration

and utilization. However, impurities are present in the newly prepared $LiFePO_4$, and the performance of the prepared battery is not stable [11,12]. In relative terms, the current recycling technologies for recovering spent $LiFePO_4$ cathode materials are mainly based on the hydrometallurgy process by acid leaching, including inorganic acids of sulfuric acid, hydrochloric acid, phosphoric acid, nitric acid, and organic acids of citric acid, oxalic acid, ascorbic acid, etc. [13–23]. The hydrometallurgy process is practiced by most $LiFePO_4$ recycling enterprises because of its low cost. However, a large amount of acid is consumed, a large amount of salt-containing wastewater needs to be treated, and iron phosphate ($FePO_4$, 95%), the main component of $LiFePO_4$, is not recycled, resulting in a waste of resources.

In recent years, some combined methods, such as the acid-free leaching process and salt roasting with water leaching, have been proposed to preferentially extract Li from spent $LiFePO_4$ cathode materials [24–27]. The core concept of the acid-free approach is to selectively transfer a majority of Li (>90%) into a water-soluble chlorate [28], sulfate [29], and Fe and P as nonsoluble oxides or precipitates. Nevertheless, the selective separation of Li and Fe is not sufficient during leaching and has significant issues that need to be solved before the method can be utilized on an industrial scale. Furthermore, the leaching kinetics of such methods are relatively slow; for example, Li from cathode materials is only totally converted to lithium chlorate or lithium sulfate with reaction times >6 h [24,28]. Moreover, fluoride ions will be enriched in the leaching solution in the Li-rich leach solution after oxidative acid leaching treatment [30]. In order to reduce fluoride ion emissions, a low-temperature thermal pretreatment process was also proposed for treating LiFePO4 cathode scrapes [31]. Selective extraction has been widely used to separate valuable metals by homogeneous reactors and hydrothermal synthesis in recent years, which could enhance mass transfer and accelerate chemical reactions [32]. Jenni Lie et al. reported the leaching of valuable metals from spent lithium-ion battery cathode powders in subcritical water extraction under optimum conditions using 0.5 $mol \cdot L^{-1}$ ascorbic acid at 100 °C with a 10 $g \cdot L^{-1}$ solid–liquid ratio within 30 min [33,34]. Liu et al. discovered that more than 98% of REEs can be leached from roasted spent Nd-Fe-B magnet materials with a roasting pretreatment by pressure leaching [35]. However, selective extraction of Li from $LiFePO_4$ cathode scrapes by oxidation roasting followed by low-acid pressure leaching has not been reported previously.

This current study proposes a novel $LiFePO_4$ recycling method that uses an oxidation-roasting pretreatment followed by low-acid pressure leaching to selectively extract lithium in a homogeneous reactor. Via this process, almost all of the lithium present can be selectively converted into water-soluble lithium sulfate within only 30 min, while Fe and P remain in the form of insoluble stable compounds. Moreover, in this process, battery-grade Li_2CO_3 can be obtained without the requirement for further complicated separation and purification procedures; currently, the demand for lithium-battery materials for Li_2CO_3 as raw materials is increasing. Another advantage is that harmful gases are removed in the oxidation-roasting process, and $FePO_4 \cdot 2H_2O$ in leaching residues with a complete crystalline form can be achieved. Therefore, this study aimed to selectively recover Li to separate Fe from spent $LiFePO_4$ cathode materials, which could be promising in industrial applications.

Compared with direct leaching of sulfuric acid and hydrogen peroxide, low-acid pressure leaching of calcine was carried out in this study. Free oxidizing agents, such as hydrogen peroxide, reduce the amount of acid and the discharge of salt-containing wastewater. Meanwhile, the electrolytes coated on the surfaces of lithium iron phosphate cathode powders are almost all decomposed after roasting, and the contact angle of the surface of the cathode materials becomes small. The hydrophilicity of the cathode materials is improved, the adhesion between the cathode materials and the reaction vessel is avoided during the reaction process, and the reaction speed is accelerated. The existence of pressure is conducive to the crystal formation of $FePO_4 \cdot 2H_2O$, and the recovery rates of the P and Fe resources are improved.

2. Materials and Methods

2.1. Materials and Characterization

A company in southern China working in the recycling business of batteries and accumulators provided the input materials used in this research. The spent $LiFePO_4$ cathode had been subjected to a pretreatment—dismantling, sieving, and grinding—and was used in the experiments as received. The mean particle size was measured by a Malvern Mastersizer 3000 (Malvern-Instruments-Ltd, Marvin, UK) and was 15.1 μm. The morphology images of the spent $LiFePO_4$ cathode materials measured by field emission scanning electron microscopy (SEM, MLA650F, FEl, Thermo Fisher Scientific Corporation, Waltham, Massachusetts, USA) are shown in Figure 1. All chemicals, including H_2SO_4, Na_2CO_3, and NaOH, were of analytical grade. All the solutions used in this study were prepared with ultrapure water (electrical conductivity < 0.055 $\mu s \cdot cm^{-1}$). The average mass fraction of the cathode materials was measured by inductively coupled plasma–optical emission spectrometry (ICP-OES, PerkinElmer Optima 7100 DV, PerkinElmer Corporation, Massachusetts, USA). The trace impurities in the rich lithium leachate were measured by inductively coupled plasma source mass spectrometry (ICPMSMS, Agilent8800, Agilent Corporation, Santa Clara, California, USA), and the contents of C were measured by a carbon–sulfur analyser (EMIA-820 V, Horiba, HORIBA Corporation, Kyoto, Japan), as shown in Table 1. The main mineral phases of the spent $LiFePO_4$ materials and leaching residues were identified by XRD (PANalytical X'Pert Pro Powder, PANalytical, Almelo, The Netherlands) using a CuKα radiation source with a 40 kV acceleration potential and current of 40 mA. XRD diffractograms were analysed by using HighScore 4.0 Plus software (Malvern Panalytical Company, Malvern, UK). The spent $LiFePO_4$ materials are consistent with $LiFePO_4$ (standard PDF card JCPDS#83-2092), as shown in Figure 2.

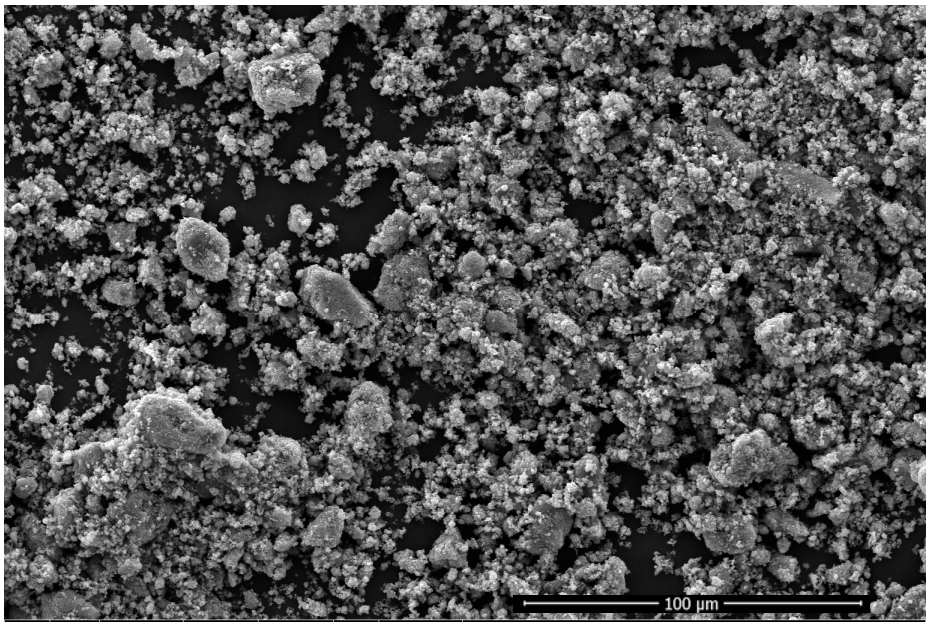

Figure 1. SEM images of the spent $LiFePO_4$ cathode materials.

Table 1. The main composition of the spent $LiFePO_4$ cathode (mass fraction, %).

Elements	Li	Fe	C	P	Cu	Al
wt %	4.18	33.26	4.63	19.56	<0.001	0.17

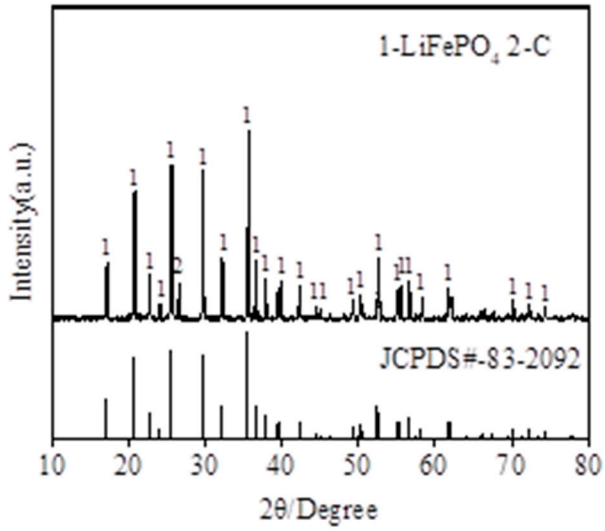

Figure 2. X-ray diffraction patterns of the spent $LiFePO_4$ cathode materials.

2.2. Experimental Procedures

2.2.1. Oxidation Roasting

The raw materials were implemented in a horizontal tube furnace (GSL-1600X, HF-Kejing, Hefei Kejing Materials Technology Co., Ltd., Hefei, China), and the temperature was measured by a K-type thermocouple controlled by a Keithley 2000 multimeter intelligent temperature controller (accuracy of ±1 °C, Tektronix, Inc., Beaverton, OR, USA). The experiments were conducted with a preset temperature (400–700 °C) at a heating rate of 10 °C·min^{-1} and with an airflow of 400 mL·min^{-1}, and the samples were placed in an Al_2O_3 crucible prior to insertion into the cold furnace. The crucibles were removed and cooled at room temperature after oxidation roasting. The phase changes before and after roasting can be characterized by XRD analysis.

2.2.2. Low-Acid Pressure-Leaching Process

The low-acid pressure-leaching experiments of roasted materials were conducted in a 100 mL cylindrical stainless homogeneous reactor (maximum temperature limit: 200 °C, maximum pressure limit: 1.0 MPa). The low-acid leaching experiments of roasted materials were performed by mixing the roasted materials and a certain concentration of a sulfuric acid solution at a predetermined L/S ratio in a 100 mL cylindrical stainless homogeneous reactor. After the reactor was heated to the set temperature for a certain time, the heating was stopped, and the reactor was naturally cooled to room temperature. After leaching, the slurry was vacuum filtered, the filtrate was collected, and its volume was recorded. The leachate was sampled and analysed to calculate the leaching of Li and Fe. The leaching residues obtained were also characterized to confirm the elemental content, the main phases, and their morphology.

The extraction of Li and Fe (%E) was calculated based on the solution samples via Equation (1):

$$\%E = (C_i \times V)/(m_o \times w_o) \times 100\% \quad (1)$$

where m_o (g) and w_o (%) are the mass of the cathode materials and the compositions of element (i) after the oxidation-roasting transformation of the waste cathode materials, respectively, and V and C_i are the volume of the leaching solution and the concentration of element (i).

2.2.3. Preparation of Lithium Carbonate

The lithium-rich solution obtained from the leaching process was first purified by adjusting the pH to 5–6 with 3 mol·L^{-1} NaOH followed by filtering to remove precipitated impurities, such as Fe and Al. Then, the pH of the solution was further adjusted to

12 to remove other minor impurities. Lithium in the leachate was first concentrated to 25 g·L^{-1} by evaporation, and the concentrated solution was added dropwise into a saturated sodium carbonate solution with a fixed molar ratio of Na_2CO_3:Li^+ = 0.6:1 at 95 °C to produce lithium carbonate. The products were washed with 95 °C ultrapure water three times and then dried at 105 °C in a drying oven for 6 h. The purity of Li_2CO_3 and the contents of the impurities were measured according to the methods proposed by the Standardization Administration of the PRC, including acid–base titration, AAS, and ICP–OES [36]. The particle size distribution of Li_2CO_3 was analysed with a Malvern Mastersizer 3000 (Malvern-Instruments-Ltd, Marvin, UK).

3. Results and Discussion

To achieve efficient leaching of lithium from the spent $LiFePO_4$ cathode materials, the stable $LiFePO_4$ cathode materials are first oxidized and roasted to convert them into a soluble phase. After that, Li can be separated from roasted cathode materials by low-acid pressure leaching without the introduction of any oxidant.

3.1. Oxidation Roasting of Spent $LiFePO_4$ Cathode Materials

3.1.1. Effect of Roasting Temperature

The effect of roasting temperature on the raw materials was investigated in detail within 60 min, as seen in Figure 3. The colour change of the roasted materials was grey when the roasting temperature was below 550 °C. The $LiFePO_4$ cathode materials gradually became brick red as the roasting temperature increased. The reason might be the oxidation of Fe^{2+} to Fe^{3+} during the roasting process. Meanwhile, the XRD results also verified this speculation, as shown in Figure 4. The temperature can drastically increase the degree of oxidation, and temperatures below 550 °C are not sufficient to achieve the complete oxidation of the raw materials in the present study. When the temperature reached 550 °C, the cathode materials were almost all oxidized to $Li_3Fe_2(PO_4)_3$ and Fe_2O_3. This result is consistent with the XRD analysis results of Zheng et al. [14] and Yafei Jie et al. [33]. However, as the temperature further increased, the diffraction peak of both $Li_3Fe_2(PO_4)_3$ and Fe_2O_3 changed slightly. Therefore, 550 °C was selected as the temperature for the oxidation roasting of spent $LiFePO_4$ cathode materials. The main reaction that occurred is shown in Equation (2) [14,33].

$$12LiFePO_4 + 3O_2 = 4Li_3Fe_2(PO_4)_3 + 2Fe_2O_3 \quad (2)$$

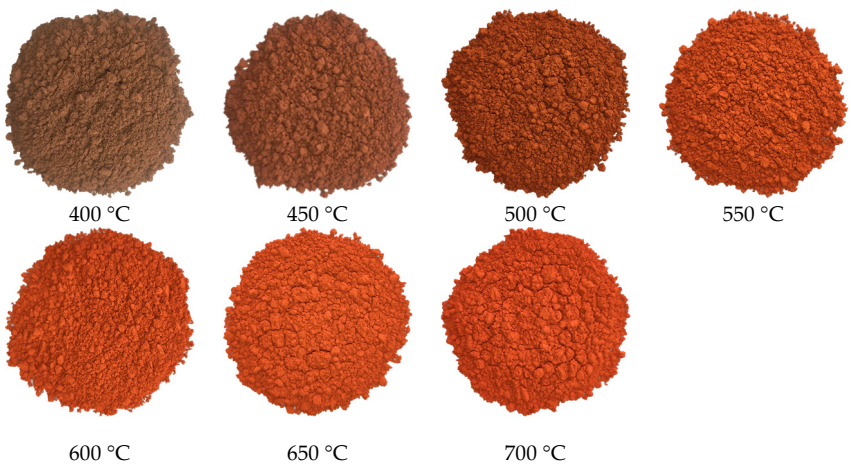

Figure 3. Images of the spent $LiFePO_4$ cathode materials at different roasting temperatures.

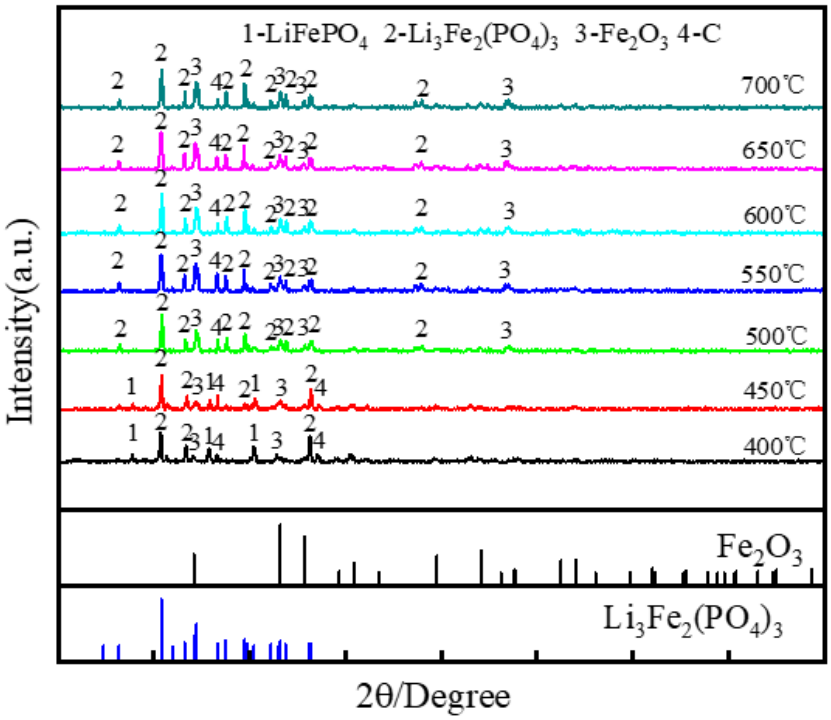

Figure 4. X-ray diffraction patterns of the spent $LiFePO_4$ cathode materials at different roasting temperatures.

3.1.2. Effect of Roasting Time

The effect of roasting time on cathode materials was investigated at 550 °C with an airflow of 50 mL·min^{-1}. The results (shown in Figure 5) indicate that the roasting time can drastically increase the degree of oxidation and that a roasting time within 60 min is not sufficient to achieve the complete oxidation of the raw materials in the present study. The cathode materials were almost all oxidized to $Li_3Fe_2(PO_4)_3$ and Fe_2O_3 when the roasting time was up to 60 min, which is consistent with the XRD analysis results (shown in Figure 6). However, as the roasting time further increased, the diffraction peak of both $Li_3Fe_2(PO_4)_3$ and Fe_2O_3 changed slightly. Therefore, 60 min was chosen as the optimum roasting time for the oxidation roasting of spent $LiFePO_4$ cathode materials.

Figure 5. Images of the spent $LiFePO_4$ cathode materials at different roasting times.

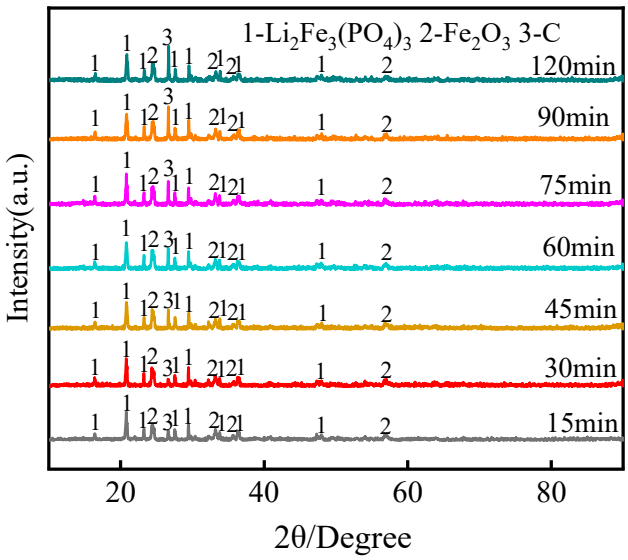

Figure 6. X-ray diffraction patterns of the spent $LiFePO_4$ cathode materials at different roasting times.

3.2. Leaching of Roasted $LiFePO_4$ Cathode Materials

Following the roasting of $LiFePO_4$ cathode materials at 550 °C within 60 min, the roasted materials were subjected to low-acid pressure leaching to achieve the selective separation of Li from the roasted materials.

3.2.1. Effect of H_2SO_4 Concentration

The effect of the H_2SO_4 acid concentration (0.2–0.7 mol·L^{-1}) on the leaching of Li and Fe was investigated at 110 °C with an S/L ratio of 150 g·L^{-1} within 60 min, and the results are shown in Figure 7. The leaching of Li increased from 64.56 to 96.45% as the H_2SO_4 concentration increased from 0.2 to 0.5 mol·L^{-1} (corresponding to an initial pH from 1.08 to 0.53), although a further increase in the H_2SO_4 concentration from 0.5 to 0.7 mol·L^{-1} resulted in only minor changes in the extraction of Li. Different from the leaching behaviour of Li, the dissolution of Fe was found to be only minor (<0.03%) when the H_2SO_4 concentration was <0.5 mol·L^{-1} because the formation of $FePO_4{\cdot}2H_2O$ (Ksp = 1.30 × 10^{-22} at 25 °C) always remained low [37,38]. However, with a further increase in the acid concentration between 0.5 mol·L^{-1} and 0.7 mol·L^{-1} (corresponding to an initial pH from 0.53 to 0.26), the extraction of Fe is only slightly increased from 0.003 to 0.22%. In contrast, the leaching efficiency of Li remained nearly constant at approximately 96% over the H_2SO_4 concentration range. The reason for the increase in Fe leaching is attributed to the dissolution of $FePO_4{\cdot}2H_2O$ at higher acid concentrations. Figure 8 shows that the iron phosphate begins to dissolve when the pH is less than 1.5, and with a further decrease in pH to 1.0, nearly 90% of the iron phosphate is dissolved into the solution. The XRD results (Figure 9) show that the leaching residues obtained at the optimal H_2SO_4 concentration are mainly composed of $FePO_4{\cdot}2H_2O$.

3.2.2. Effect of Leaching Temperature

The effect of temperature on the leaching of Li and Fe was examined by varying the temperature from 80 to 130 °C with an H_2SO_4 concentration of 0.5 mol·L^{-1} at an S/L ratio of 150 g·L^{-1} within 60 min. The results, shown in Figure 10, indicate that the leaching efficiency of Li increased substantially from 64 to 96.45% as the reaction temperature increased from 80 to 110 °C. However, a further increase in leaching temperature to between 110 and 130 °C leads to a slight decrease in Li extraction due to the rapid precipitation of $FePO_4{\cdot}2H_2O$ crystals, and some lithium ions are lost by entrainment. Different from Li, the extraction of Fe decreased obviously, from 20.0% to 0.03%, with an increase in the leaching temperature from 80 to 100 °C. However, with a further increase in the leaching

temperature between 100 and 130 °C, the extraction of Fe changes slightly. This is mainly because increasing the temperature is beneficial to the formation of iron phosphate. Under these conditions, Fe and P precipitated as $FePO_4 \cdot 2H_2O$, and Li almost completely remained in the pregnant solution. The results shown in Figure 11 verified that the precipitation efficiency of $FePO_4 \cdot 2H_2O$ increased gradually in the pregnant solution in the range of 80 to 130 °C. The reason can be understood in the following manner. At the early stage, the precipitation of $FePO_4 \cdot 2H_2O$ was amorphous, resulting in a relatively low precipitation efficiency due to its high solubility. As the reaction proceeds, the amorphous precipitate with a disordered arrangement transforms into a thermodynamically stable phase of crystalline precipitate to decrease the embodied energy [33]. Since the leaching of Li peaked at 96.45% at a temperature of 110 °C, this temperature was chosen for further experiments. However, there is a slight influence on the leaching of Li and Fe as the temperature is in the range of 100 to 130 °C. The results also illustrate that the selective separation of Li and Fe could be achieved mainly because of the experiments performed by pressure leaching, which had little influence on the concentration of H_2SO_4 and the reaction time. The leaching residues are also mainly composed of $FePO_4 \cdot 2H_2O$, Fe_2O_3, and C, as shown in Figure 12. When the reaction temperature is below 100 °C, the XRD diffraction peaks of Fe_2O_3 are weak, while the peaks are stronger at temperatures above 100 °C. It can also verify that the higher temperature was also helpful to the more complete crystal form of $FePO_4 \cdot 2H_2O$.

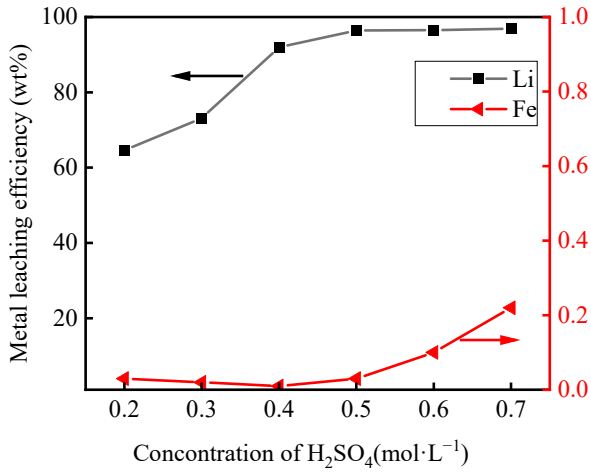

Figure 7. Effect of H_2SO_4 concentration on the leaching efficiency of Li and Fe from roasted materials (T = 110 °C; t = 60 min; S/L = 150 g·L^{-1}).

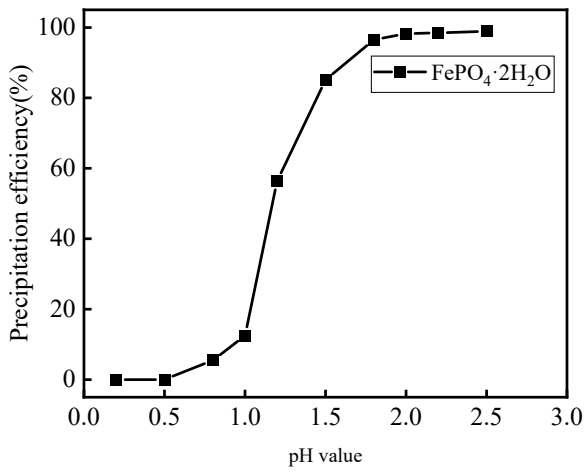

Figure 8. Effect of pH on dissolution of $FePO_4 \cdot 2H_2O$ S/L = 150 g·L^{-1}). ($C_{Fe} = C_P$ = 0.2 mol·L^{-1}, T = 30 °C; t = 60 min).

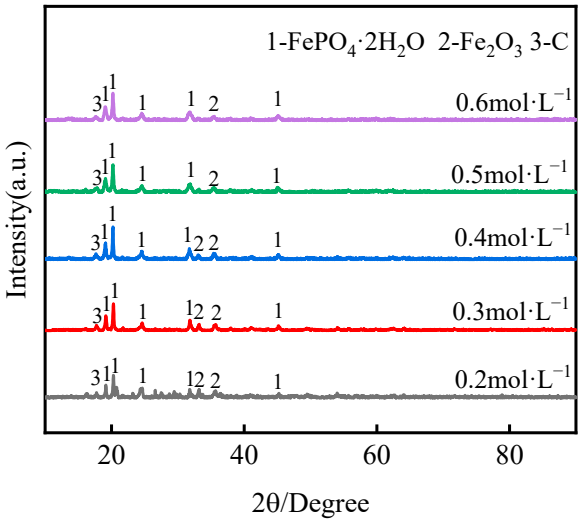

Figure 9. X-ray diffraction patterns of the leach residues at 0.5 mol·L^{-1} H_2SO_4 (T = 110 °C; t = 60 min; S/L = 150 g·L^{-1}).

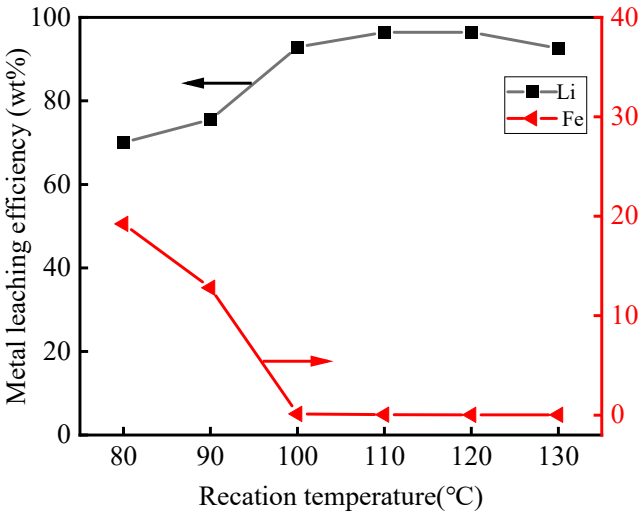

Figure 10. Effects of reaction temperature on the leaching efficiency of Li and Fe from roasted materials (C = 0.5 mol·L^{-1}; t = 60 min; S/L = 150 g·L^{-1}).

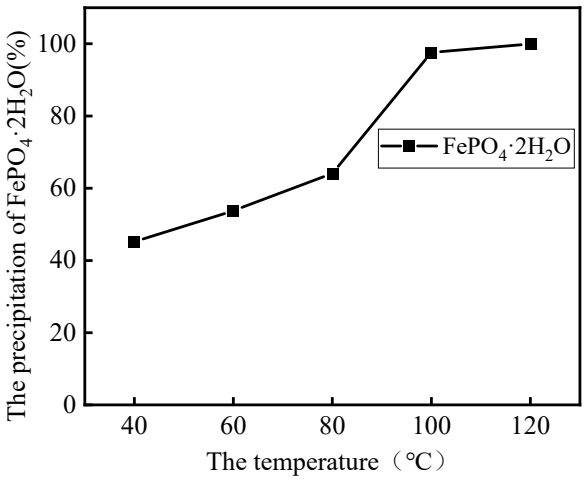

Figure 11. Effects of reaction temperature on the precipitation rate of *t* = 60 min and S/L =150 g·L^{-1}, $FePO_4{\cdot}2H_2O$ (C_{Fe} = C_P = 0.2 mol·L^{-1}, initial pH = 0.5; *t* = 60 min).

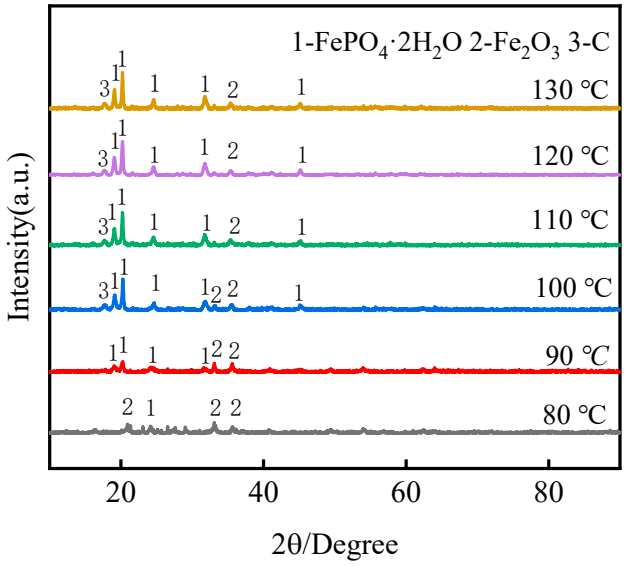

Figure 12. X-ray diffraction patterns of the leach residues from different reaction temperatures.

3.2.3. Effect of Leaching Time

The effect of leaching time was investigated in a range from 30 to 120 min. The other conditions were as follows: H_2SO_4 concentration of 0.5 mol·L^{-1}, leaching temperature of 110 °C, and solid-to-liquor (S/L) ratio of 150 g·L^{-1}. As shown in Figure 13, the leaching time caused no obvious change in the leaching efficiency of Li and Fe. Even when the leaching time was 30 min, the leaching efficiency of Li could reach 91.95% and that of Fe could be as low as 0.01%. Li and Fe could be almost selectively separated completely in the range of 30 to 150 min studied. Due to the best separating effect of Li and Fe at a leaching time of 60 min, this time was chosen for further experiments. When the reaction time was less than 30 min, the XRD diffraction peak of $FePO_4{\cdot}2H_2O$ was not obvious, and that of Fe_2O_3 decreased gradually, as shown in Figure 14. This illustrated that crystals of $FePO_4{\cdot}2H_2O$ grow more completely and that Fe_2O_3 is gradually dissolved by acid when the time is longer than 60 min.

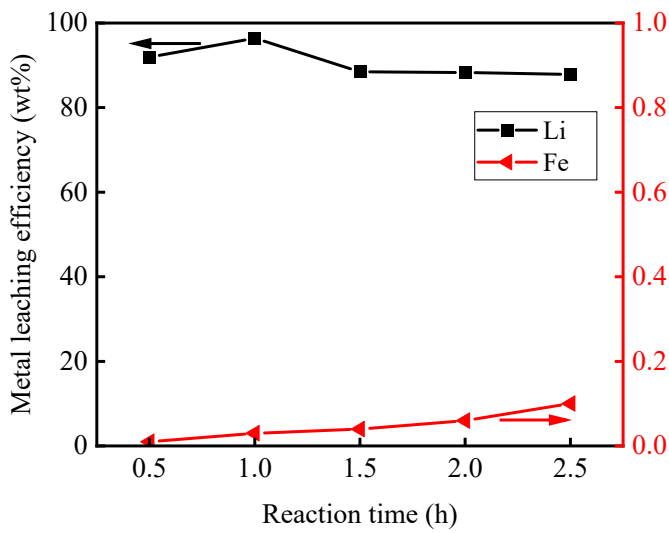

Figure 13. Effect of reaction time on the leaching efficiency of Li and Fe from roasted materials (T = 110 °C; *C* = 0.5 mol·L^{-1}; S/L = 150 g·L^{-1}).

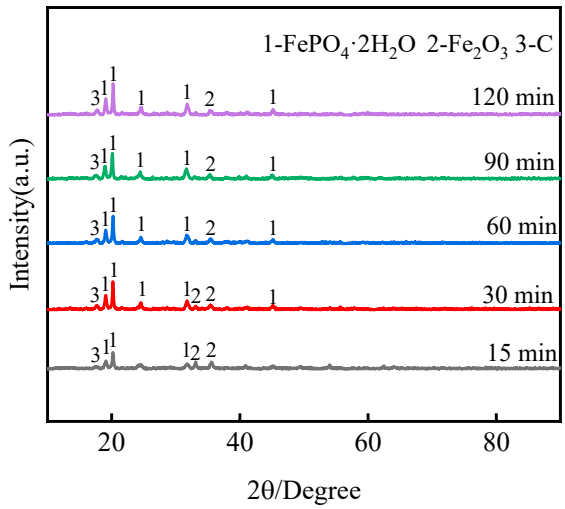

Figure 14. X-ray diffraction patterns of the leach residues from different reaction times.

3.2.4. Effect of the Solid-to-Liquor (S/L) Ratio

The effect of the solid-to-liquor (S/L) ratio was investigated in a range from 50 to 250 g·L^{-1}. The other leaching conditions were as follows: H_2SO_4 concentration of 0.5 mol·L^{-1}, leaching temperature of 110 °C, and leaching time of 60 min. As shown in Figure 15, when the solid-to-liquor (S/L) ratio increased in the whole studied range, and as more H_2SO_4 was added, the total volume of the leaching solution increased. The solid-to-liquor (S/L) ratio obviously affected the leaching efficiency of Li, and the Li leaching efficiency rose from 62.92 to 96.45% as the S/L ratio increased in the range of 50 to 150 g·L^{-1}. However, the leaching efficiency of Fe remained relatively stable at a low level of 0.08%. When the S/L ratio was 250 g·L^{-1}, the leaching efficiency of Fe reached 0.08%. To make the volume of the leaching solution as low as possible to reduce the following evaporation costs and decrease the additional amount of H_2SO_4, an S/L ratio of 150 g·L^{-1} was selected for further experiments. It was apparent that the appropriate addition amount of H_2SO_4 was very low compared to its theoretical value (experimental ratio of 150 g·L^{-1} vs. theoretical ratio of 150 g·L^{-1}). As a result, the alkali amount added in the following experiments on impurity removal can be decreased. The XRD diffraction peaks of $FePO_4 \cdot 2H_2O$ and Fe_2O_3 are slightly weaker than those under the other conditions when S/L is 50 g·L^{-1}, as shown in Figure 16. It could be that the quantities of $FePO_4 \cdot 2H_2O$ and Fe_2O_3 are less than when the additional amount of H_2SO_4 is insufficient.

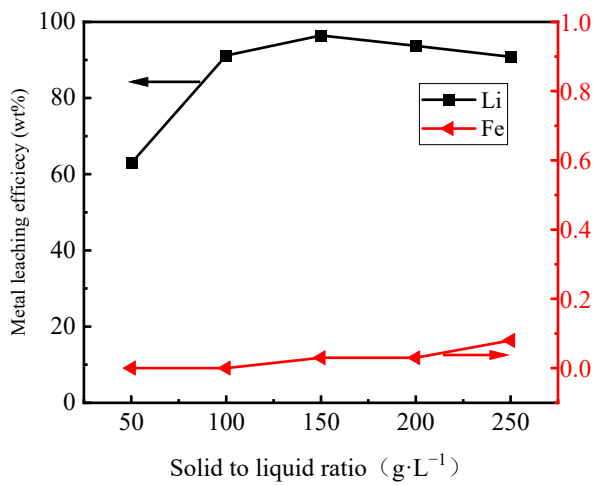

Figure 15. Effects of solid-to-liquid ratio on the leaching efficiency of Li and Fe from roasted materials (T = 110 °C; C = 0.5 mol·L^{-1}; t = 60 min).

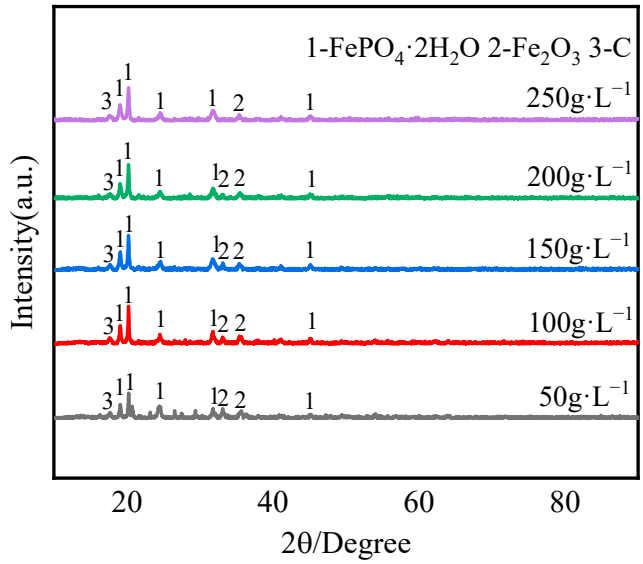

Figure 16. X-ray diffraction patterns of the leaching residues from different solid-to-liquid ratios.

3.3. Li_2CO_3 Products

The concentrations of Fe^{3+}, Al^{3+}, and Cu^{2+} were 16 mg·L^{-1}, 6 mg·L^{-1} and 3.2 mg·L^{-1}, respectively, in the leachate from the low-acid pressure-leaching process under optimum conditions. Then, NaOH solution with 3 mol·L^{-1} was added to adjust the pH = 6, and impurities, such as Al^{3+}, Fe^{3+} and Cu^{2+}, were further removed. After filtration, the concentration of Fe^{3+}, Al^{3+} and Cu^{2+} were 3.5 m mg·L^{-1}, 1.8 mg·L^{-1} and 1.5 mg·L^{-1} in the leachate, respectively. Then, the pH was adjusted to 12 to remove the other impurities such as Mg, while the content for Fe^{3+}, Al^{3+} and Cu^{2+} were almost unchanged at a pH from 6 to 12. Subsequently, the purified leach solution was evaporated to a high concentration (25 g·L^{-1}), and the content of minor impurities for Ca^{2+}, Mg^{2+}, K^{+}, Pb^{2+}, and Cl^{-} was almost undetectable. The purified, Li-rich solution then underwent carbonation with saturated Na_2CO_3 to prepare Li_2CO_3, and the products were washed three times with ultrapure water after filtration.

Under optimum conditions of 95 °C using the purified Li-rich solution (25 g·L^{-1}) obtained from the purification process, Li recovery is up to 87.5%, a level that is significantly higher than that previously reported for solvent extraction or evaporation followed by carbonation (ca. 75–85%) [39,40]. The purity of the final Li_2CO_3 products is presented in Table 2, which can also meet the requirements of battery-grade materials. In comparison, most of the Li_2CO_3 produced by other methods, with a purity of 90.0%, does not meet the standards needed for battery-grade Li_2CO_3 [40], which indicates that additional cleaning processes are necessary to improve the purity of Li_2CO_3. The SEM image (Figure 17) illustrates that the obtained Li_2CO_3 was composed of agglomerated blocks in which the particle size distribution was measured to be approximately 6.5 microns. The final products are consistent with Li_2CO_3 (standard PDF card JCPDS#87-0728), as shown in Figure 18.

Table 2. The composition of the products of Li_2CO_3 (wt%).

Element	Li	Fe	Cu	Al	Mg	Ca
Standard Values	99.5	0.001	0.0003	0.001	0.008	0.02
Measured Values	99.7	0.0006	0.0002	0.0004	-	-
Element	**Na**	**K**	**Pb**	**SO_4^{2-}**	**Cl^{-}**	**Hydrochloric Acid Insoluble Matter**
Standard Values	0.04	0.01	0.002	0.08	0.003	0.05
Measured Values	0.03	-	-	0.05	-	0.01

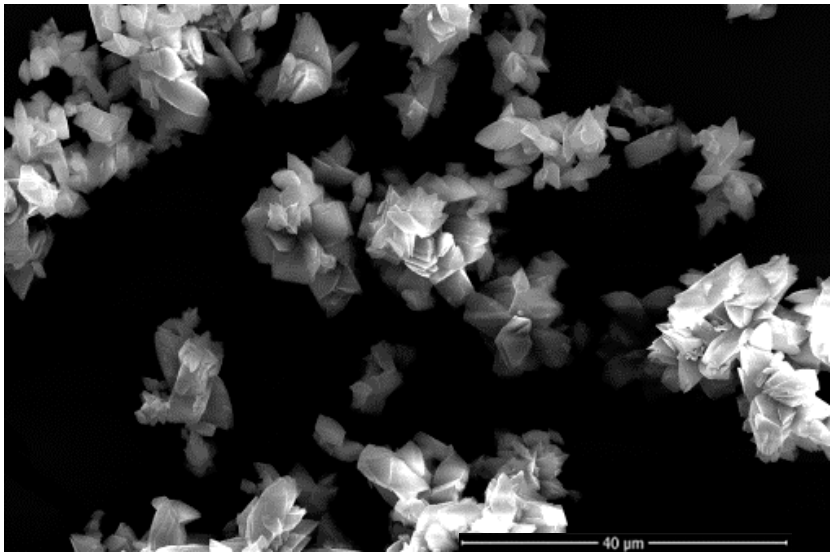

Figure 17. SEM images of the obtained Li_2CO_3 products.

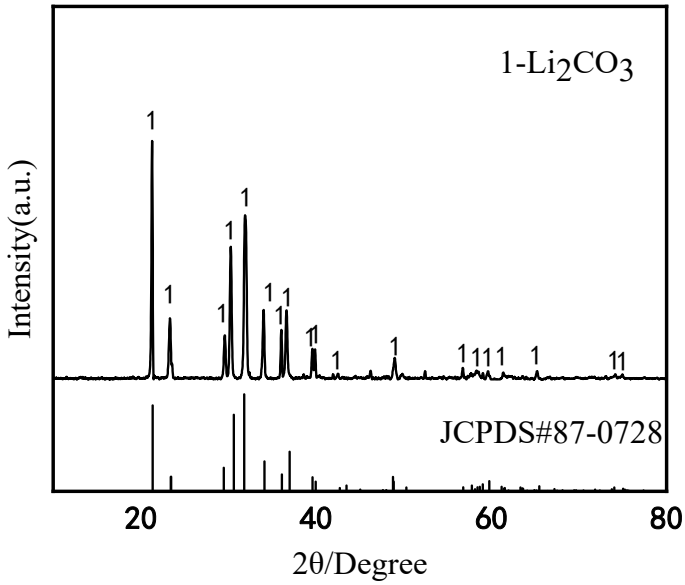

Figure 18. X-ray diffraction patterns of the obtained Li_2CO_3 products.

3.4. Analysis of Leaching Residues

After drying, the residues were measured by XRD, which was well matched with the standard pattern of $FePO_4 \cdot 2H_2O$, Fe_2O_3, and C, as discussed in the previous chapter, which demonstrated that Fe precipitated as $FePO_4 \cdot 2H_2O$ and Fe_2O_3 in the leaching residues. Therefore, Fe was recovered in the forms of $FePO_4 \cdot 2H_2O$ and Fe_2O_3. These results agree well with the previous publication, while the residues shown were different morphologies at 90 °C and 110 °C, as can be observed in the SEM images (Figure 19a,c). The shapes of crystallized $FePO_4 \cdot 2H_2O$ were lower at 90 °C than at 110 °C, as shown in Figure 19b,d [41]. The content of Li was fairly low, while the contents of Fe, P, and O were very high, as seen in Figure 20. It can be confirmed that Li was almost entirely in the leaching solution, which is consistent with the previous section.

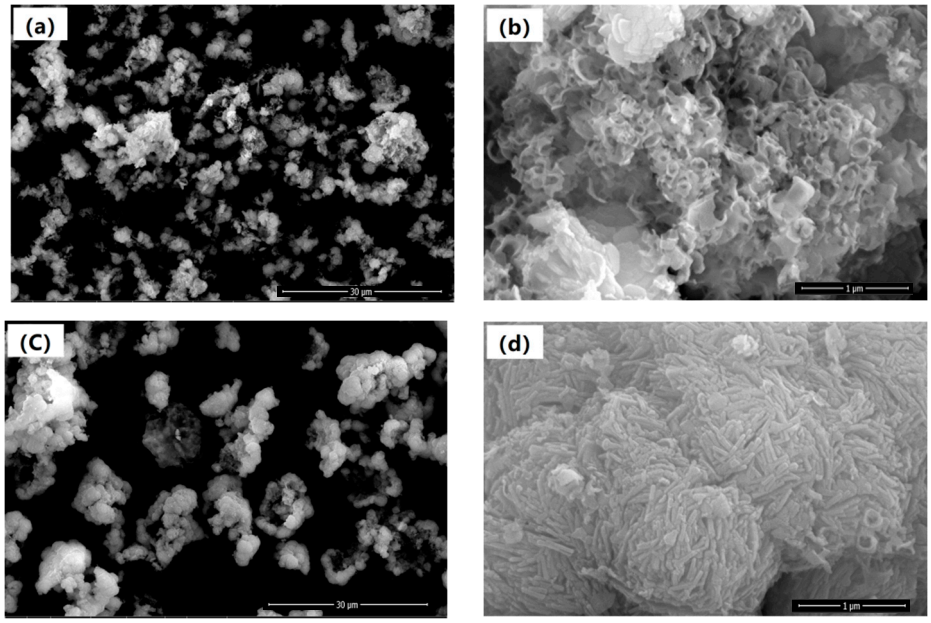

Figure 19. SEM images of residue samples obtained from different leaching temperatures: (**a**) 90 °C; (**b**) 90 °C, magnified; (**c**) 110 °C; and (**d**) 110 °C, magnified.

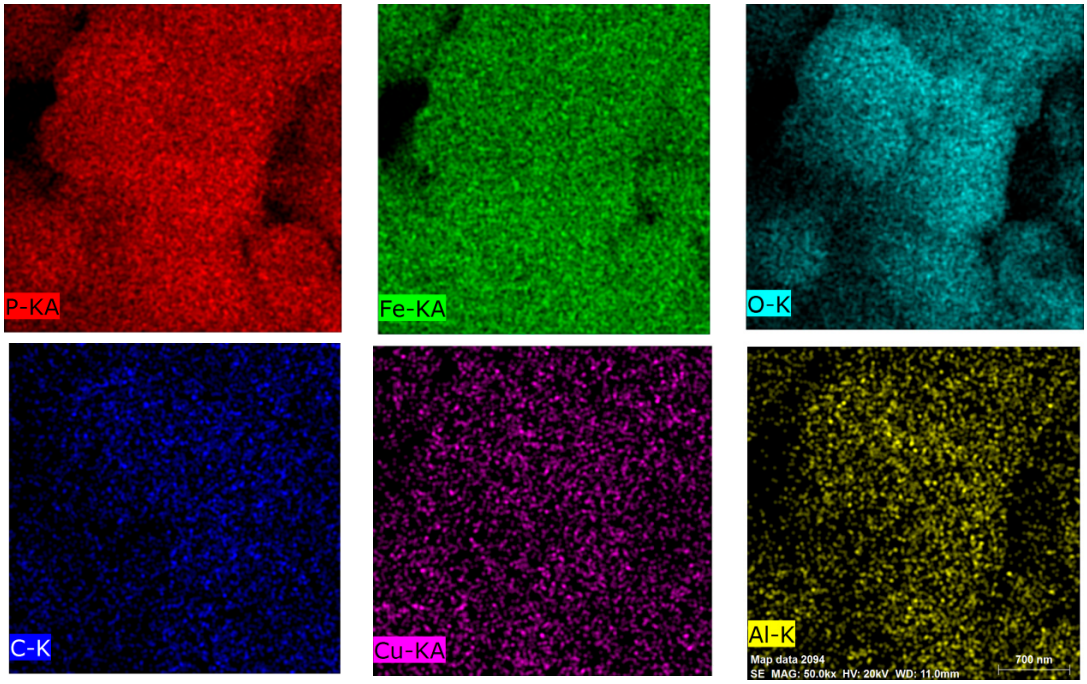

Figure 20. Elemental maps of the leaching residues in the local area.

3.5. Flowsheet Development

From the above results, a new process for the selective separation and recovery of Li from spent $LiFePO_4$ batteries by oxidation roasting followed by low-acid pressure leaching is outlined, and the mass balance of the valuable metals throughout the recovery process is shown in Figure 21. The composition of the raw materials and byproducts obtained from the proposed flowsheet are shown in Table 3. The application of the current process could significantly improve the separation and recovery of Li and Fe from spent $LiFePO_4$ cathode materials. This research provides a reference case for the selective separation and recovery of Li from spent $LiFePO_4$ batteries. For the roasted materials followed by low-acid leaching in a homogeneous reactor, the lithium-rich solution obtained can be further used to remove

impurities by preparing battery-grade Li_2CO_3, whereas the leaching residue byproduct can be used to prepare $FePO_4$ products.

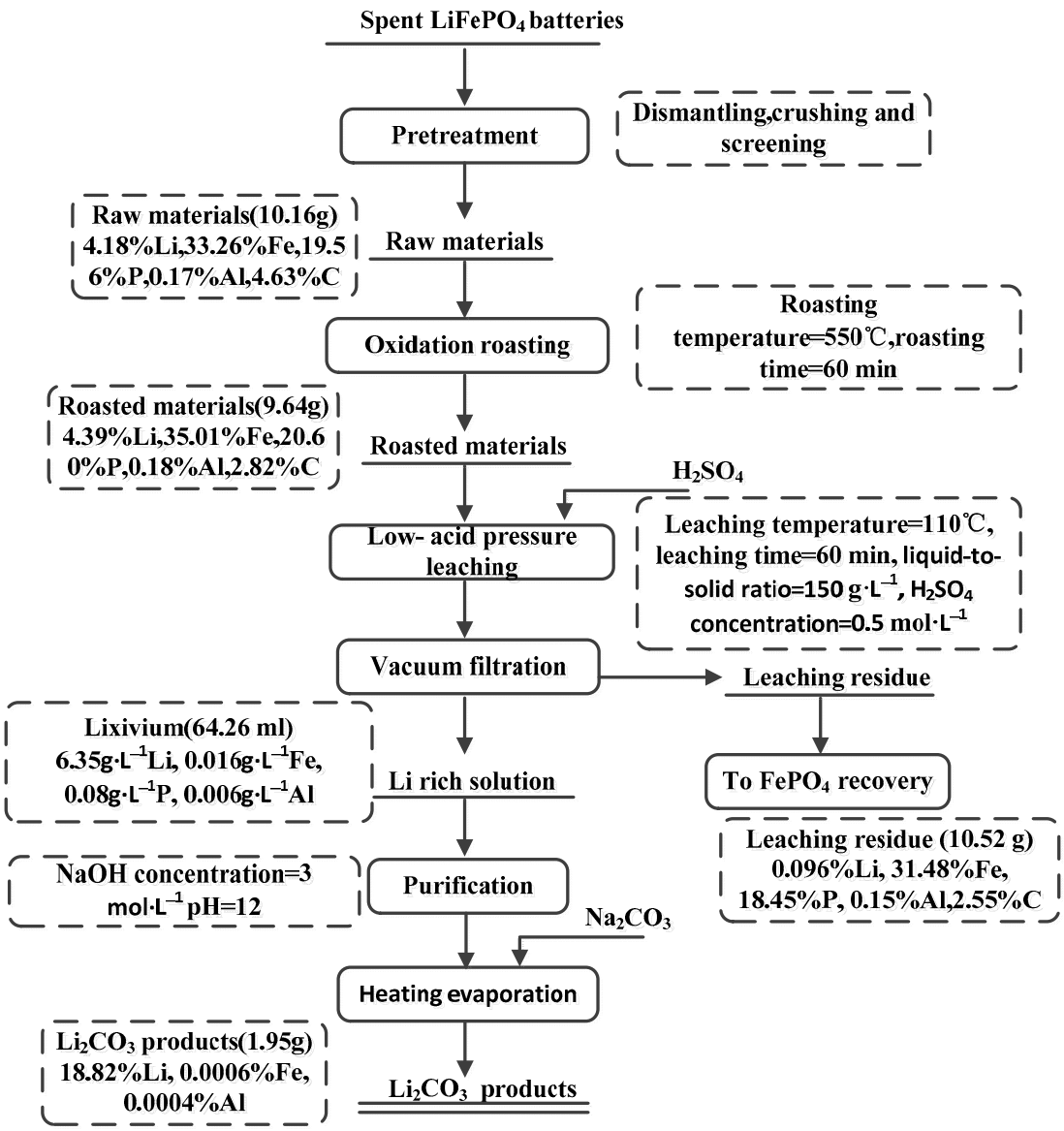

Figure 21. Proposed flowsheet for the selective recovery of Li from spent $LiFePO_4$ cathode materials.

Table 3. Elemental composition of raw materials and byproducts obtained from the proposed flowsheet.

Samples Description and Units of Elemental Assay	Li	Fe	Al	P	C	Sample Mass (g) or Volume (mL)
Raw materials (%*w*/*w*)	4.18	33.26	0.17	19.56	4.63	10.16
Roasted materials (%*w*/*w*)	4.39	35.01	0.18	20.60	2.82	9.64
Lixivium($g \cdot L^{-1}$)	6.35	0.016	0.006	0.08	-	64.26
Li_2CO_3 products (%*w*/*w*)	18.82	0.0006	0.0004	-	-	1.95
Leaching residue (%*w*/*w*)	0.096	31.48	0.15	18.45	2.55	10.52

3.6. The Economic Analysis of the Proposed Process

The economic analysis was conducted by spotting the local market prices for the bulk amount of the chemicals in China, as shown in Table 4. The costs for total raw materials, chemical reagents and products were approximately USD 1915, USD 20.9264, and USD 2764.71, respectively. The products for the Li_2CO_3 weighing 95.96 kg and the byproducts for leaching the residue weighing 517.71 kg could be recycled from spent $LiFePO_4$ cathode materials of 500 kg. Consequently, a net revenue of approximately USD 601.5186 can be obtained by the current recycling process, in which only raw materials, the reagent cost, and the product values were considered. The cost of equipment, water consumption, labour costs, and factory construction costs are ignored.

Table 4. Raw materials, chemical reagent, and product prices to treat 500 kg of spent $LiFePO_4$ cathode materials by the present green process in China.

Substance	Price (USD/kg^{-1})	Consumption (kg)	Economic Benefits (USD)
Raw materials	3.83	500	−1915
H_2SO_4	0.041	162.72	−6.671
NaOH	0.82	0.47	−0.3854
Na_2CO_3	0.38	36.5	−13.87
Leaching residue	0.547	517.71	283.19
Li_2CO_3 products	25.86	95.96	2481.52

The current recycling process can be divided into five parts: oxidation roasting; low-acid pressure leaching; filtering, drying, and sieving; purification and evaporation; and precipitation. The economic feasibility based on the energy consumption of the present recycling process is subsequently calculated. The consumption of energy per unit operation to treat 500 kg of spent $LiFePO_4$ cathode materials is considered in Table 5. With respect to the mass balance of the main elements from the flow sheet presented in Figure 21, such an example may vary with the change in parameters and operational conditions, such as the scale of treatment. The energy consumption is mainly electric power consumption, and the total energy consumption and the cost of energy are 2085 kWh and USD 172 in this process, respectively, according to the local energy price in China.

Table 5. The energy consumption to treat 500 kg of spent $LiFePO_4$ cathode materials for adopting this recycling process in China.

Process	Price (USD/kWh)	Energy Cost (kWh)	Total Price (USD)
Oxidation roasting	0.109	750	81.75
Low-acid pressure leaching	0.109	562.5	61.3125
Filtering, drying, and sieving	0.109	357.5	38.9675
Purification and evaporation	0.109	240	26.16
Precipitation	0.109	175	19.075
Total		2085	227.265

Finally, the total dealing revenue in this study was calculated as USD 601.5186, with a 500 kg scale of spent $LiFePO_4$ cathode materials in China. Such an economic analysis of the proposed process is clearly in favour of being greener and more economically attractive in the recovery of Li_2CO_3 products from the $LiFePO_4$ cathode material industrial solid wastes.

4. Conclusions

This research proposes an efficient method to selectively separate Li and Fe from spent $LiFePO_4$ cathode materials. The results show that:

(1) Through the selective recovery of Li and Fe by oxidation roasting following low-acid pressure leaching, the spent $LiFePO_4$ cathode materials were oxidized to $Li_3Fe_2(PO_4)_3$

and Fe_2O_3, the remaining electrolyte and some of the carbon in the raw materials decomposed, and the selective extraction of Li was achieved by carbonated water leaching. The results showed that it was more effective and efficient in the selective separation of Li and Fe than the conventional method;

(2) Under optimal conditions, by a low-acid pressure-leaching process using 0.5 mol·L^{-1} H_2SO_4 at 110 °C with a 150 g·L^{-1} S/L ratio, >96% Li was extracted, and, within 60 min, the leaching process could be adapted to a wide range of pH values. The reaction temperature played a significant role in the selective recovery of Li and Fe from roasted materials and the phase of $FePO_4 \cdot 2H_2O$ in leaching residues;

(3) Oxidation roasting following the pressure-leaching process showed the advantages of higher efficiency, shorter reaction time, and lower acid concentrations needed. Economic and energy consumption analyses clearly show that this recycling process has great potential to become industrially viable. It has very good potential as an alternative process for spent $LiFePO_4$ recycling.

Author Contributions: Literature search, Z.C. and C.S.; study design, Z.C. and F.L.; investigation, C.S.; data collection, Z.C. and C.S.; data analysis, Z.C. and C.S.; data interpretation, Z.C.; writing, Z.C. and F.L.; review and editing, F.L. and J.W. All authors have read and agreed to the published version of the manuscript.

Funding: This paper has been financially supported by the Training Plan for Academic and Technical Leaders of Major Disciplines in Jiangxi Province (20225BCJ23009), Unveiling and commanding project in Jiangxi Province (20213AAE02010), Postdoctoral Innovative Talent Support Program of Shandong Province and Program of Qingjiang Excellent Young Talents, Jiangxi University of Science and Technology (No. JXUSTQJYX2019006), Jiangxi Postdoctoral Science Foundation (No. 2019 KY07), Natural Science Foundation for Distinguished Young Scholars of Jiangxi Province (No.20232ACB214006), Jiangxi Provincial Key Laboratory of Flash Green Development and Recycling (No. 20193BCD40019), and Academic and Technical Leaders of Major Disciplines in Jiangxi Province (20213BCJ22003).

Data Availability Statement: The data presented in this study are available upon request from the corresponding author. The data are not publicly available due to privacy.

Conflicts of Interest: The authors declare no conflict of interest. The funders had no role in the design of the study; in the collection, investigation, analysis, or interpretation of data; in the writing of the manuscript; or in the decision to publish the results.

References

1. Yu, W.H.; Guo, Y.; Shang, Z.; Zhang, Y.C.; Xu, S.M. A review on comprehensive recycling of spent power lithium-ion battery in China. *Transportation* **2022**, *11*, 100155. [CrossRef]
2. Fan, M.C.; Zhao, Y.; Kang, Y.Q.; Wozny, J.; Liang, Z.; Wang, J.X.; Zhou, G.M.; Li, B.H.; Tavajohi, N.; Kang, F.Y. Room-temperature extraction of individual elements from charged spent $LiFePO_4$ batteries. *Rare Met.* **2022**, *41*, 1595–1604. [CrossRef]
3. Li, L.; Bian, Y.; Zhang, X.; Yao, Y.; Xue, Q.; Fan, E.; Wu, F.; Chen, R. A green and effective room-temperature recycling process of $LiFePO_4$ cathode materials for lithium-ion batteries. *Waste Manag.* **2019**, *85*, 437–444. [CrossRef] [PubMed]
4. Wang, X.; Wang, X.; Zhang, R.; Wang, Y.; Shu, H. Hydrothermal preparation and performance of $LiFePO_4$ by using Li_3PO_4 recovered from spent cathode scraps as Li source. *Waste Manag.* **2018**, *78*, 208–216. [CrossRef] [PubMed]
5. Natarajan, S.; Aravindan, V. Burgeoning prospects of spent lithium-ion batteries in multifarious applications. *Adv. Energy Mater.* **2018**, *8*, 1802303. [CrossRef]
6. Harper, G.; Sommerville, R.; Kendrick, E.; Driscoll, L.; Slater, P.; Stolkin, R.; Walton, A.; Christensen, P.; Heidrich, O.; Lambert, S.; et al. Recycling lithium-ion batteries from electric vehicles. *Nature* **2019**, *575*, 75–86. [CrossRef]
7. Zeng, X.; Li, J.; Singh, N. Recycling of spent lithium-ion battery: A Critical Review. *Crit. Rev. Environ. Sci. Technol.* **2014**, *44*, 1129–1165. [CrossRef]
8. Wu, J.; Mackenzie, A.; Sharma, N. Recycling lithium-ion batteries: Adding value with multiple lives. *Green Chem.* **2020**, *22*, 2244–2254. [CrossRef]
9. Yu, J.; Wang, X.; Zhou, M.; Wang, Q. A redox targeting-based material recycling strategy for spent lithium ion batteries. *Energy Environ. Sci.* **2019**, *12*, 2672–2677. [CrossRef]
10. Song, X.; Hu, T.; Liang, C.; Long, H.L.; Zhou, L.; Song, W.; You, L.; Wu, Z.S.; Liu, J.W. Direct regeneration of cathode materials from spent lithium iron phosphate batteries using a solid phase sintering method. *RSC Adv.* **2017**, *7*, 4783. [CrossRef]
11. Wang, L.H.; Li, J.; Zhou, H.M.; Huang, Z.Q.; Tao, S.D.; Zhai, B.K.; Liu, L.Q.; Hu, L.S. Regeneration cathode material mixture from spent lithium iron phosphate batteries. *J. Mater. Sci. Mater. Electron.* **2018**, *29*, 9283–9290. [CrossRef]

12. Li, X.L.; Zhang, J.; Song, D.W.; Song, J.S.; Zhang, L.Q. Direct regeneration of recycled cathode material mixture from scrapped $LiFePO_4$ batteries. *J. Power Sources* **2017**, *345*, 78–84. [CrossRef]
13. Li, H.; Xing, S.; Liu, Y.; Li, F.; Guo, H.; Kuang, G. Recovery of lithium, iron, and phosphorus from spent $LiFePO_4$ batteries using stoichiometric sulfuric acid leaching system. *ACS Sustain. Chem. Eng.* **2017**, *5*, 8017–8024. [CrossRef]
14. Zheng, R.; Zhao, L.; Wang, W.; Liu, Y.; Ma, Q.; Mu, D.; Li, R.; Dai, C. Optimized Li and Fe recovery from spent lithium-ion batteries via a solution-precipitation method. *RSC Adv.* **2016**, *6*, 43613–43625. [CrossRef]
15. Yang, Y.X.; Zheng, X.H.; Cao, H.B.; Zhao, C.L.; Lin, X.; Ning, P.G.; Zhang, Y.; Jin, W.; Sun, Z. A closed-loop process for selective metal recovery from spent lithium iron phosphate batteries through mechanochemical activation. *ACS Sustain. Chem. Eng.* **2017**, *5*, 9972–9980. [CrossRef]
16. Yan, T.T.; Zhong, S.W.; Zhou, M.M.; Guo, X.M.; Hu, J.W.; Wang, F.F.; Zeng, F.T.; Zuo, S.C. High efficiency method for recycling lithium from spent $LiFePO_4$ cathode. *Nanotechnol. Rev.* **2020**, *9*, 1586–1593. [CrossRef]
17. Jin, H.; Zhang, J.L.; Yang, C.; Ma, L.L.; Chen, Y.Q.; Wang, C.Y. Selective recovery of lithium from spent $LiFePO_4$ battery via a self-catalytic air oxidation method. *Chem. Eng. J.* **2023**, *460*, 141805. [CrossRef]
18. Liu, K.; Wang, M.M.; Zhang, Q.Z.; Xu, Z.B.; Labianca, C.; Komarek, M.; Gao, B.; Tsang, C.W. A perspective on the recovery mechanisms of spent lithium iron phosphate cathode materials in different oxidation environments. *J. Hazard. Mater.* **2023**, *445*, 130502. [CrossRef]
19. Jin, H.; Zhang, J.L.; Wang, D.D.; Jing, Q.K.; Chen, Y.Q.; Wang, C.Y. Facile and efficient recovery of lithium from spent $LiFePO_4$ batteries via air oxidation–water leaching at room temperature. *Green Chem.* **2022**, *24*, 152. [CrossRef]
20. Zhang, B.L.; Qu, X.; Chen, X.; Liu, D.X.; Zhao, Z.Q.; Xie, H.W.; Wang, D.H.; Yin, H.Y. A sodium salt-assisted roasting approach followed by leaching for recovering spent $LiFePO_4$ batteries. *J. Hazard. Mater.* **2022**, *424*, 127586. [CrossRef]
21. Yang, Y.X.; Meng, X.Q.; Cao, H.B.; Lin, X.; Liu, C.M.; Sun, Y.; Zhang, Y.; Sun, Z. Selective recovery of lithium from spent lithium iron phosphate batteries: A sustainable process. *Green Chem.* **2018**, *20*, 3121–3133. [CrossRef]
22. Fan, E.; Li, L.; Zhang, X.; Bian, Y.; Xue, Q.; Wu, J.; Wu, F.; Chen, R. Selective recovery of Li and Fe from spent lithium-ion batteries by an environmentally friendly mechanochemical approach. *ACS Sustain. Chem. Eng.* **2018**, *6*, 11029–11035. [CrossRef]
23. Peng, C.; Liu, F.P.; Wang, Z.; Wilson, B.P.; Lundström, M. Selective extraction of lithium (Li) and preparation of battery grade lithium carbonate (Li_2CO_3) from spent Li-ion batteries in nitrate system. *J. Power Sources* **2019**, *415*, 179–188. [CrossRef]
24. Dai, Y.; Xu, Z.D.; Hua, D.; Gua, H.N.; Wang, N. Theoretical-molar Fe^{3+} recovering lithium from spent $LiFePO_4$ batteries: An acid-free, efficient, and selective process. *J. Hazard. Mater.* **2020**, *396*, 122707. [CrossRef]
25. He, K.; Zhang, Z.Y.; Zhang, F.S. A green process for phosphorus recovery from spent $LiFePO_4$ batteries by transformation of delithiated $LiFePO_4$ crystal into $NaFeS_2$. *J. Hazard. Mater.* **2020**, *395*, 122614. [CrossRef] [PubMed]
26. Zhang, J.L.; Hu, J.T.; Liu, Y.B.; Jing, Q.K.; Yang, C.; Chen, Y.Q.; Wang, C.Y. Sustainable and facile method for the selective recovery of lithium from cathode scrap of spent $LiFePO_4$ batteries. *ACS Sustain. Chem. Eng.* **2019**, *7*, 5626–5631. [CrossRef]
27. Wang, Y.Q.; An, N.; Wen, L.; Wang, L.; Jiang, X.T.; Hou, F.; Yin, Y.X.; Liang, J. Recent progress on the recycling technology of Li-ion batteries. *J. Energy Chem.* **2021**, *55*, 391–419. [CrossRef]
28. Liu, K.; Tan, Q.Y.; Liu, L.L.; Li, J.H. Acid-Free and Selective Extraction of Lithium from Spent Lithium Iron Phosphate Batteries via a Mechanochemically Induced Isomorphic Substitution. *Environ. Sci. Technol.* **2019**, *53*, 9781–9788. [CrossRef] [PubMed]
29. Liu, K.; Liu, L.L.; Tan, Q.Y.; Li, J.H. Selective extraction of lithium from a spent lithium iron phosphate battery by mechanochemical solid-phase oxidation. *Green Chem.* **2021**, *23*, 1344–1352. [CrossRef]
30. Jie, Y.F.; Yang, S.H.; Shi, P.F.; Chang, D.; Fang, G.; Mo, C.X.; Ding, J.; Liu, Z.Q.; Lai, Y.Q.; Chen, Y.M. Thermodynamic Analysis and Experimental Investigation of Al and F Removal from Sulfuric Acid Leachate of Spent $LiFePO_4$ Battery Powder. *Metals* **2021**, *11*, 1641. [CrossRef]
31. Bi, H.J.; Zhu, H.B.; Zu, L.; Gao, Y.; Gao, S.; Peng, J.L.; Li, H.B. Low-temperature thermal pretreatment process for recycling inner core of spent lithium iron phosphate batteries. *Waste Manag. Res.* **2020**, *39*, 146–155. [CrossRef]
32. Lin, E.Y.; Rahmawati, A.; Ko, J.H.; Liu, J.C. Extraction of yttrium and europium from waste cathode-ray tube (CRT) phosphor by subcritical water. *Sep. Purif. Technol.* **2018**, *192*, 166–175. [CrossRef]
33. Jie, Y.F.; Yang, S.H.; Li, Y.; Zhao, D.Q.; Lai, Y.Q.; Chen, Y.M. Oxidizing Roasting Behavior and Leaching Performance for the Recovery of Spent $LiFePO_4$ Batteries. *Minerals* **2020**, *10*, 949. [CrossRef]
34. Jie, Y.F.; Yang, S.H.; Li, Y.; Hu, F.; Zhao, D.Q.; Chang, D.; Lai, Y.Q.; Chen, Y.M. Waste Organic Compounds Thermal Treatment and Valuable Cathode Materials Recovery from Spent $LiFePO_4$ Batteries by Vacuum Pyrolysis. *ACS Sustain. Chem. Eng.* **2020**, *8*, 19084–19095. [CrossRef]
35. Liu, F.P.; Porvalib, A.; Wang, J.L.; Wang, H.Q.; Peng, C.; Wilsonb, B.P.; Lundström, M. Recovery and separation of rare earths and boron from spent Nd-Fe-B magnets. *Miner. Eng.* **2020**, *145*, 106097. [CrossRef]
36. SAC. *Methods for Chemical Analysis of Lithium Carbonate, Lithium Hydroxide Monohydrate and Lithium Chloride*; Standardization Administration of the People's Republic of China: Beijing, China, 2013.
37. Xiao, C.; Zeng, L.; Li, Y.B.; Xiao, L.S. Thermodynamic analysis on removing iron by phosphate precipitation. *Chin. J. Nonferrous Met.* **2018**, *28*, 637–643.
38. Jing, Q.K.; Zhang, J.L.; Liu, Y.B.; Yang, C.; Ma, B.Z.; Chen, Y.Q.; Wang, C.Y. E-pH Diagrams for the Li-Fe-P-H_2O System from 298 to 473 K: Thermodynamic Analysis and Application to the Wet Chemical Processes of the $LiFePO_4$ Cathode Material. *J. Phys. Chem. C* **2019**, *123*, 14207–14215. [CrossRef]

39. Guo, X.; Cao, X.; Huang, G.; Tian, Q.; Sun, H. Recovery of lithium from the effluent obtained in the process of spent lithium-ion batteries recycling. *J. Environ. Manag.* **2017**, *198*, 84–89. [CrossRef]
40. Chen, X.; Chen, Y.; Zhou, T.; Liu, D.; Hu, H.; Fan, S. Hydrometallurgical recovery of metal values from sulfuric acid leaching liquor of spent lithium-ion batteries. *Waste Manag.* **2015**, *38*, 349–356. [CrossRef]
41. Lou, W.B.; Zhang, Y.; Zhang, Y.; Zheng, S.L.; Sun, P.; Wang, X.J.; Qiao, S.; Li, J.Z.; Zhang, Y.; Liu, D.Y.; et al. A facile way to regenerate $FePO_4 \cdot 2H_2O$ precursor from spent lithium iron phosphate cathode powder: Spontaneous precipitation and phase transformation in an acidic medium. *J. Alloys Compd.* **2021**, *856*, 158148. [CrossRef]

Disclaimer/Publisher's Note: The statements, opinions and data contained in all publications are solely those of the individual author(s) and contributor(s) and not of MDPI and/or the editor(s). MDPI and/or the editor(s) disclaim responsibility for any injury to people or property resulting from any ideas, methods, instructions or products referred to in the content.